



ELSEVIER

Contents lists available at SciVerse ScienceDirect

Talanta

journal homepage: [www.elsevier.com/locate/talanta](http://www.elsevier.com/locate/talanta)

# Efficient immobilization of glucose oxidase by in situ photo-cross-linking for glucose biosensing

Guanglei Fu<sup>b</sup>, Zhifei Dai<sup>a,b,\*</sup><sup>a</sup> Department of Biomedical Engineering, College of Engineering, Peking University, Beijing 100871, People's Republic of China<sup>b</sup> Nanomedicine and Biosensor Laboratory, School of Life Science and Engineering, Harbin Institute of Technology, Harbin 150001, People's Republic of China

## ARTICLE INFO

## Article history:

Received 18 February 2012

Received in revised form

26 April 2012

Accepted 30 April 2012

Available online 8 May 2012

## Keywords:

Glucose oxidase

Biosensor

Self-assembly

Diazo-resin

Prussian blue

Multi-walled carbon nanotubes

## ABSTRACT

A glucose biosensor was fabricated based on electrostatic self-assembly in combination with in situ photo-cross-linking of glucose oxidase (GOx) and diazo-resin–chitosan (DAR–CS) on Prussian blue deposited multi-walled carbon nanotubes (PB-MWNTs) backbone. It was demonstrated that GOx was initially ionically deposited and subsequently covalently photo-cross-linked onto the PB-MWNTs backbone using photo-sensitive DAR–CS as the assembly interlayer. The modified electrode exhibited good electrical conductivity and effective electron transfer mediation toward H<sub>2</sub>O<sub>2</sub> reduction due to the employment of PB-MWNTs as the fabrication backbone. The biosensor showed high sensitivity of 77.9 μA mM<sup>-1</sup> cm<sup>-2</sup> to glucose in the linear concentration range from 1.0 × 10<sup>-5</sup> to 1.1 × 10<sup>-3</sup> M with fast response time of 10 s, detection limit of 3.1 × 10<sup>-6</sup> M, and good anti-interference ability. More importantly, the biosensor exhibited greatly improved biosensing stability in comparison with the non-photo-cross-linked biosensor attributed to the conversion of weak ionic bonds to strong covalent ones for enzyme immobilization by the proposed strategy. The results for glucose determination in real serum samples with the biosensor were found to be in good agreement with those obtained by the conventional clinical procedure.

© 2012 Elsevier B.V. All rights reserved.

## 1. Introduction

The electrochemical biosensors have attracted intensive research interests because of their potential applications in many fields [1]. The procedure of enzyme immobilization on transducer with proper electrochemical materials remains a crucial step for construction of enzyme-based biosensors [2,3]. The electrostatic self-assembly technique is particularly advantageous to construct molecularly ordered enzyme architectures on solid interfaces [4,5], which offers many striking advantages, such as mild processing conditions, precise control of composition, and simplicity of procedure [6]. However, ionically bound enzymes have to be confronted with the problem of enzyme leakage when changes in pH, ionic strength or temperature occur during measurements [7], leading to poor stability of biosensors.

The electrostatic self-assembly technique in combination with the photo-cross-linking technique has emerged as an efficient approach to fabricate stable covalently attached assemblies [6,8,9]. The procedure involves only two steps: first, electrostatic self-assembly between photosensitive cross-linkers such as diazo-resin (DAR) and target components; second, conversion of the resulting weak ionic

bonds to strong covalent ones by “cross-linking” via in situ photo-reaction. Photo-cross-linked assemblies have been proven to exhibit increased resistance to solvent etching, and to result in denser and more rigid films [10]. Hence, the combination of the electrostatic self-assembly technique with the photo-cross-linking technique is particularly promising for construction of stable enzyme assembly architectures on electrode surfaces. The conversion of weak electrostatic interaction between diazonium groups in DAR and carboxylate groups of nonessential amino acid residues in enzymes to covalent bonds may therefore result in stable immobilization of enzymes. However, the poor electrical conductivity and the required relatively high working potentials that could limit the sensitivity and selectivity of many biosensors remain as problems to be solved [11,12].

Prussian blue deposited carbon nanotubes hybrids (PB-CNTs), combining the facilitation effect of CNTs on electron transfer [13–16] with the low-potential electron transfer mediation effect of PB toward redox processes of many substances [17–20], hold great potential in construction of sensitive and selective biosensors. PB-CNTs can act as both the low-potential redox mediator and electron transfer facilitator as demonstrated in our previous work [21]. More importantly, the PB-CNTs forming membranes are highly three-dimensional porous as observed in previous works [21], providing an opportunity for the further assembly of large amounts of enzymes on the PB-CNTs backbone.

This paper fabricated a novel glucose biosensor based on electrostatic self-assembly in combination with in situ photo-cross-linking of glucose oxidase (GOx) as the model enzyme and

\* Corresponding author at: Department of Biomedical Engineering, College of Engineering, Peking University, Beijing 100871, People's Republic of China.

Tel./fax: +86 10 62767580.

E-mail address: zhifei.dai@pku.edu.cn (Z. Dai).

URL: <http://nanobio.hit.edu.cn/> (Z. Dai).

diazoresin–chitosan (DAR–CS) on PB deposited multi-walled CNTs (PB-MWNTs) backbone. The PB-MWNTs backbone was primarily modified on the electrode surface. GOx was then assembled onto the PB-MWNTs backbone through electrostatic interaction using photo-sensitive DAR–CS as the interlayer, followed by in situ photo-cross-linking of the composites on the backbone (Scheme 1). The electrostatic self-assembly in combination with in situ photo-cross-linking could effectively address the problem of enzyme leakage of the traditional electrostatic self-assembly method. In addition, the PB-MWNTs backbone imparts the biosensing system good electrochemical properties. Hence, in comparison with traditional biosensors constructed by the electrostatic self-assembly merely, the new biosensor combined the synergistic effects of efficient enzyme immobilization and good electrochemical properties, resulting higher stability, sensitivity and selectivity. Therefore, the proposed strategy provided a promising platform for constructing other biosensors.

## 2. Experiment

### 2.1. Reagent and materials

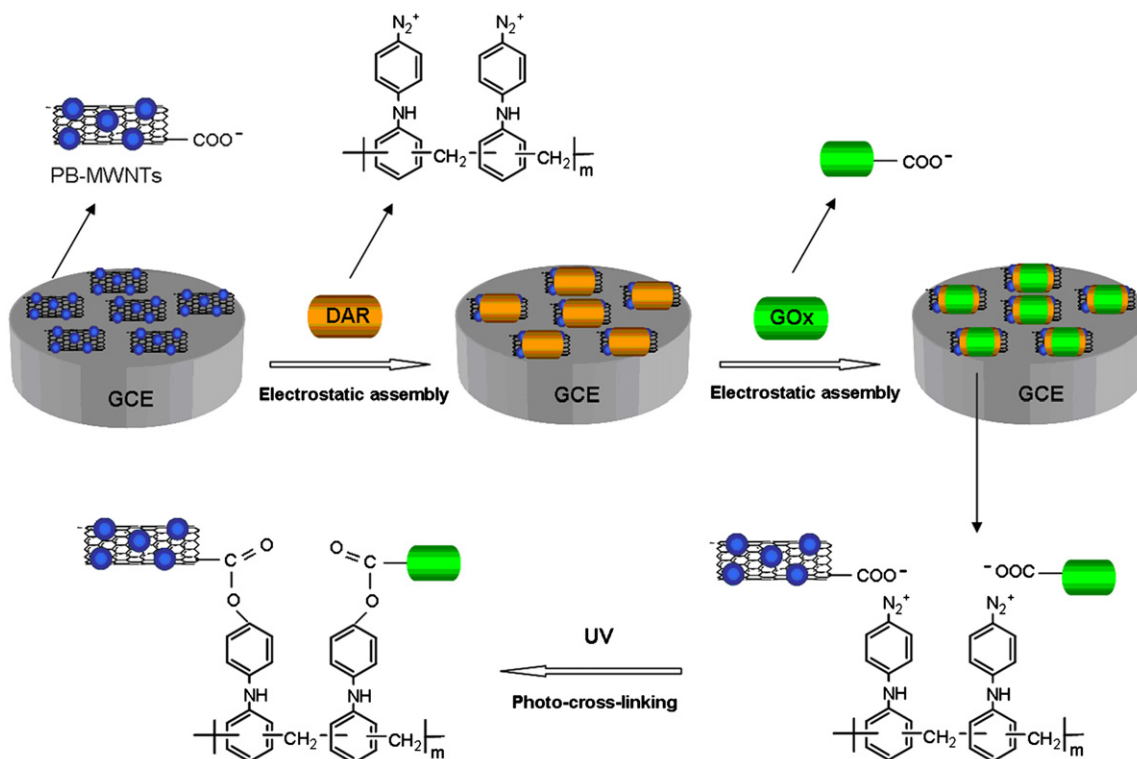
Glucose oxidase (GOx, EC 1.1.3.4, Type X-S, 158.9 units/mg, from *Aspergillus niger*), D-(+)-glucose (99.5%) and chitosan (CS, 90% deacetylation) were purchased from Sigma (USA). Carboxyl-functionalized multi-walled carbon nanotubes (MWNTs, 95%, content of carboxylic acid group 3.0 wt%, diameter 20–40 nm, length 1–2  $\mu\text{m}$ ) were purchased from Shenzhen Nanotech. Port. Co., Ltd. (Shenzhen, China). Diazoresin (DAR) was synthesized according to the method reported in the literature [6]. Phosphate buffer solution (PBS, 0.05 M, pH 6.5) containing  $\text{K}_2\text{HPO}_4$ ,  $\text{KH}_2\text{PO}_4$  and 0.1 M KCl was employed as the supporting electrolyte. Unless otherwise stated, reagents were of analytical reagent grade and used as received. Aqueous solutions were prepared with deionized water (18.2 M $\Omega$  cm) from a Milli-Q purification system.

### 2.2. Apparatus

Electrochemical measurements were performed on a PARSTAT 2273 electrochemical workstation (PE Co., USA) with a standard three-electrode system employing a platinum wire as the counter electrode, a saturated calomel electrode (SCE) as the reference electrode and a modified glassy carbon electrode (GCE) as the working electrode. The electrical impedance spectroscopy (EIS) was carried out in pH 6.5 PBS containing 10 mM  $\text{K}_3[\text{Fe}(\text{CN})_6]/\text{K}_4[\text{Fe}(\text{CN})_6]$  and 0.5 M KCl. The measurement of glucose concentration in bovine serum sample was carried out by adding the serum into the electrochemical cell with a certain volume of PBS under stirring. UV irradiation was performed using a UV lamp (365 nm). Scanning electron microscopy (SEM) measurements were made on a Quanta 200 FEG scanning electron microscope (FEI Co., USA). Absorption spectra were recorded on a Cary 4000 UV–vis spectrophotometer (USA).

### 2.3. Preparation of PB-MWNTs hybrids and DAR–CS hybrid polyelectrolyte

Prussian blue (PB) deposited Multi-walled carbon nanotubes (MWNTs) hybrids (PB-MWNTs) were synthesized according to the literature [22]. For preparation of the diazoresin (DAR)–chitosan (CS) hybrid polyelectrolyte (DAR–CS) hybrid polyelectrolyte, CS was first dissolved in 1.0% acetic acid with sonication to obtain 0.5% CS solution. After adjusting of the pH value to 5.0 with NaOH, the CS solution was then mixed with a DAR aqueous solution in a certain ratio under stirring in the dark to obtain the DAR–CS hybrid polyelectrolyte solution with final DAR and CS concentrations of 2 mg/mL and 0.15%, respectively. The hybrid polyelectrolyte solution was stored in the dark at 4  $^\circ\text{C}$  when not in use.



Scheme 1. Illustration of the preparation process of the biosensor.

## 2.4. Fabrication of the modified GCE

The GCE was successively polished to a mirror finish with 0.3 and 0.05  $\mu\text{m}$  alumina slurry followed by rinsing thoroughly with deionized water. After successive sonication in ethanol and deionized water, the electrode was dried at room temperature. 2.0 mg/mL PB-MWNTs aqueous suspension was prepared by dispersing PB-MWNTs in deionized water with sonication for 10 min. 8  $\mu\text{L}$  of the obtained suspension was then dropped on the GCE surface. After drying at room temperature, the PB-MWNTs modified GCE (PB-MWNTs-GCE) was first immersed in the DAR-CS solution for 30 min in the dark to adsorb the hybrid polyelectrolyte on the PB-MWNTs backbone, followed by thorough rinse with deionized water to obtain the DAR-CS/PB-MWNTs-GCE. The DAR-CS/PB-MWNTs-GCE was then immersed in pH 6.5 PBS containing 2.5 mg/mL GOx in the dark for 30 min to obtain the GOx/DAR-CS/PB-MWNTs-GCE. After thorough rinse with deionized water, the modified electrode was immediately exposed to a UV lamp at 365 nm with a distance of 10.0 cm for a given time to allow the photoreaction. The modified electrodes were stored at 4  $^{\circ}\text{C}$  in the dark when not in use.

## 3. Results and discussion

### 3.1. Characterization of the GOx/DAR-CS/PB-MWNTs composite film

The morphologies of the composites were characterized by SEM as shown in Fig. 1. Carboxyl-functionalized MWNTs exhibited smooth and clean surfaces (A). After the deposition of PB, a

large number of nanoparticles with diameter ranging from 10 to 20 nm were randomly deposited on MWNTs surfaces (B). Nevertheless, sufficient bare MWNTs surfaces could be still observed. The absorption peak appeared at 700 nm in the UV-vis absorption spectra (D, c) of the composites confirmed the formation of PB deposited MWNTs hybrids (PB-MWNTs) [22]. The PB-MWNTs forming membrane was uniform and highly porous as observed in the SEM image, providing an opportunity for the assembly of large amounts of enzymes onto the PB-MWNTs backbone. More importantly, the PB-MWNTs backbone modified on the electrode surface held great potential to act as both the sensitive electron transfer facilitator and the selective low-potential electron transfer mediator as demonstrated in our previous work [21]. After the electrostatic adsorption of the positively charged mixture of DAR and CS (DAR-CS), the PB-MWNTs backbone with both negatively charged PB and bare carboxyl-functionalized MWNTs was obviously wrapped with the polyelectrolyte (C). The appearance of the absorption peak at 374 nm in the UV-vis absorption spectra (D, d) of the composite film, which corresponded well with that of DAR due to the  $\pi-\pi^*$  transition of the diazonium group (D, a) [6], confirmed the adsorption of DAR onto the PB-MWNTs backbone. In addition, the hydrogen bonding interaction between the hydroxyl group and the diazonium group [23–26] could allow the co-adsorption of DAR and CS onto the PB-MWNTs backbone, which then acted as a positively charged photosensitive and biocompatible interlayer for the further electrostatic deposition of GOx. It should be noted that only negative charged enzymes could be deposited onto the DAR modified surface. GOx has an isoelectric point of is 4.2, so it is negatively charged in the used solution with a pH value of 6.5.

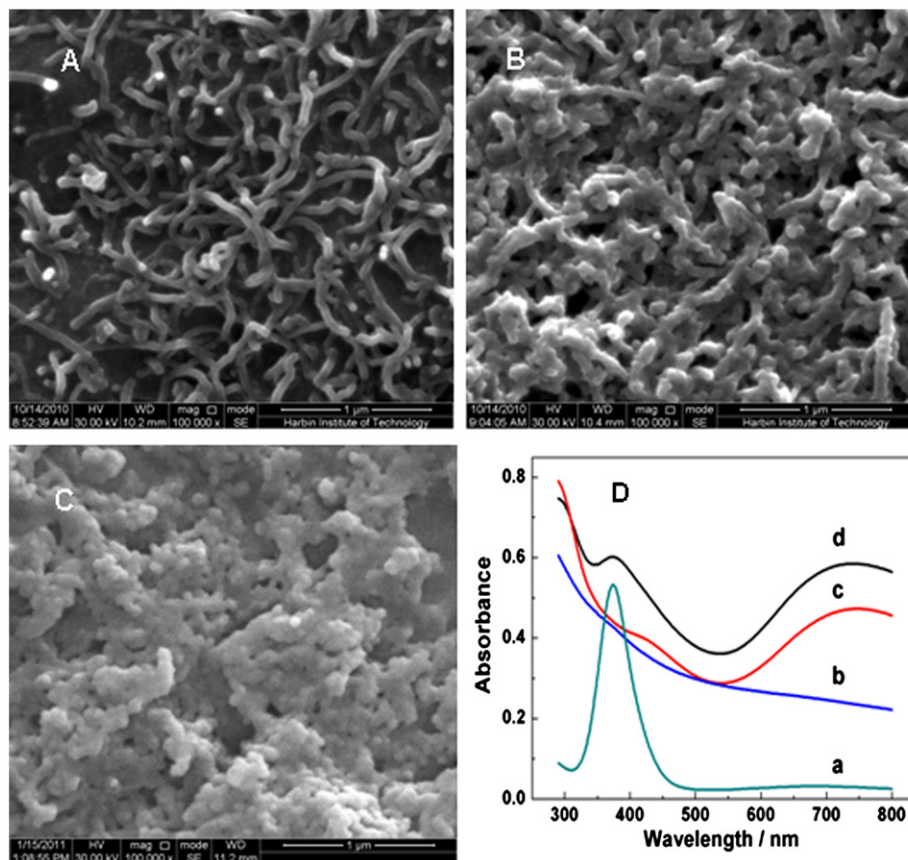


Fig. 1. Scanning electron micrographs of (A) MWNTs, (B) PB-MWNTs and (C) DAR-CS/PB-MWNTs. (D) UV-vis absorption spectra of (a) DAR, (b) MWNTs, (c) PB-MWNTs and (d) DAR-CS/PB-MWNTs composite film on a quartz slide.

### 3.2. Photo-cross-linking of the GOx/DAR-CS/PB-MWNTs composite film

DAR has been widely used as the photosensitive cross-linker to fabricate stable assemblies because of the ease of photoreaction between phenyldiazonium and carboxylate, sulfate or phenol groups due to the decomposition of the diazonium group [6]. After the electrostatic adsorption of GOx onto the surface of the DAR-CS interlayer, photoreaction occurred between phenyldiazonium groups in DAR and carboxylate groups in GOx upon UV irradiation, leading to the covalent attachment of GOx onto the PB-MWNTs backbone. However, enzymes can be denatured under UV irradiation required for the photoreaction, limiting the application of the method in enzyme immobilization. Traditionally, assemblies containing DAR were dried with  $N_2$  before UV irradiation. It was found that the  $N_2$ -dried GOx/DAR-CS/PB-MWNTs-GCE showed almost no response to glucose after exposure of the electrode surface to UV irradiation for only 20 s (the biosensing mechanism to glucose was discussed in the following section), indicating the denaturation of GOx under UV irradiation. Nevertheless, the non-dried GOx/DAR-CS/PB-MWNTs-GCE showed dramatically high response to glucose after irradiation within a certain period as shown in Fig. 2(A). More than 80% of the initial current response retained even after irradiation for 3 min, although the response decreased with the increase of the irradiation time. The result indicated that the aqueous environment on the electrode

surface played an important role in protecting enzyme activity against UV irradiation. Enzymes can form numerous hydrogen bonds with surrounding water molecules through their exposed polar and ionic groups in aqueous environment [27,28]. It is well known that H-bonding is important in stabilizing the secondary, tertiary and quaternary structures of proteins [29,30], which may prevent the denaturation of enzymes under UV irradiation to a certain extent. Hence, after rinse with deionized water, the modified electrode surfaces without drying were immediately exposed to UV irradiation for a certain time.

Photo-cross-linking in aqueous and nonaqueous environments between DAR and materials containing carboxylate groups such as heparin and carbon nanotubes has been extensively reported [6,8,10]. Herein, the photo-cross-linking of the GOx/DAR-CS/PB-MWNTs composite film on the quartz slide was performed employing UV irradiation for different time. UV-vis absorption spectroscopy was used to confirm the photoreaction as shown in Fig. 2(B). As the irradiation time increased, the absorbance at 374 nm decreased. Simultaneously, a new peak appeared at 295 nm and increased slightly. The result was in agreement with the literatures [6,9], indicating that GOx was covalently attached onto the PB-MWNTs backbone through photoreaction of phenyldiazonium in DAR with carboxylate groups in GOx due to the decomposition of the diazonium group. Therefore, this procedure converted the weak ionic bonds between DAR and GOx, as well as that between bare MWNTs (carboxyl-functionalized) and DAR, to strong covalent bonds. Under UV irradiation, DAR was converted to its phenyl cationic form after releasing  $N_2$ ; then, an SN 1 type of nuclear displacement by carboxylate groups occurred [6]. Actually, there was a possibility that the hydrogen bonds between the diazonium group in DAR and hydroxyl groups in CS also converted to covalent bonds. In consideration of both the protection of enzyme activity and the occurrence of photoreaction, a compromising irradiation time of 3 min for the modified electrodes was used in the following investigation. As a result, large amounts of GOx molecules were covalently deposited onto the PB-MWNTs backbone.

### 3.3. Electrochemical properties of the GOx/DAR-CS/PB-MWNTs composite film

Electrochemical impedance spectroscopy (EIS) has been an effective method to monitor the interfacial features of a surface to allow the understanding of processes associated with the conductive electrode surface [1]. Fig. 3 shows the typical Nyquist plots of the modified electrodes using  $K_3[Fe(CN)_6]/K_4[Fe(CN)_6]$  as the probe. The electron transfer resistance ( $R_{et}$ ) for the redox process of the probe decreased dramatically after PB-MWNTs were modified on bare GCE (b), implying that the PB-MWNTs backbone greatly facilitated the electron transfer of the probe to the electrode surface attributed mainly to the contribution of MWNTs. When DAR-CS was adsorbed on the PB-MWNTs backbone, the  $R_{et}$  increased slightly (c). After the further adsorption of GOx, the  $R_{et}$  increased obviously because GOx partially blocked the electron transfer of the probe (d). The result confirmed the successful fabrication of the GOx/DAR-CS/PB-MWNTs composite film on GCE.

Fig. 4 shows cyclic voltammograms of the GOx/DAR-CS/PB-MWNTs-GCE in pH 6.5 PBS at various scan rates. With a formal potential of +0.153 V, a pair of well-defined redox peaks appeared at each voltammogram due to the redox conversion between PB and Prussian white. Both the cathodic peak current ( $I_{pc}$ ) and the anodic peak current ( $I_{pa}$ ) were linearly dependent on the square root of the scan rate in the range from 10 to 400 mV/s, indicating a diffusion-controlled electrochemical process. The result was consistent with that of many previous works [21],

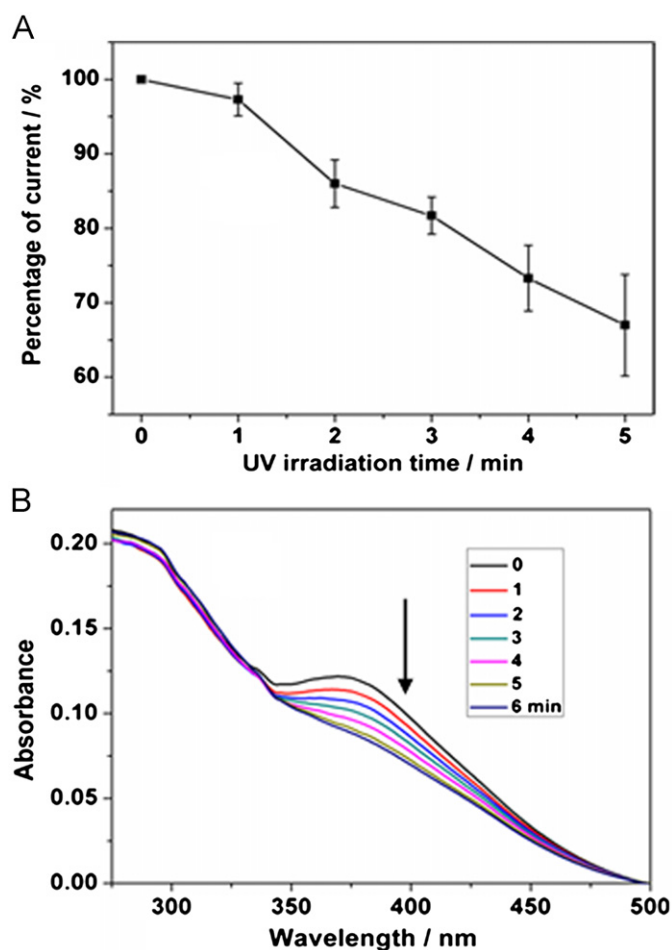


Fig. 2. (A) Effect of UV irradiation time of the GOx/DAR-CS/PB-MWNTs composite film on the electrode surface on amperometric response to 0.1 mM glucose. (B) UV-vis absorption spectra of the GOx/DAR-CS/PB-MWNTs composite film on a quartz slide upon exposure to UV irradiation for 0, 1, 2, 3, 4, 5, 6 min.

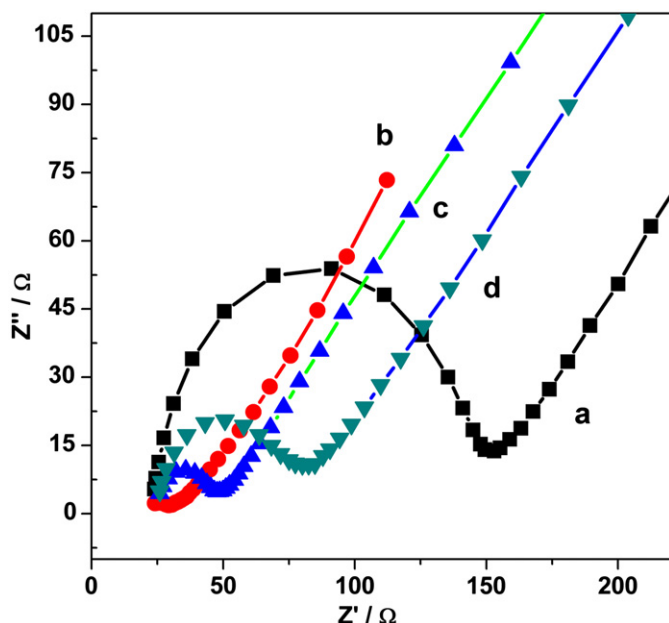


Fig. 3. Electrochemical impedance spectra (EIS) of (a) GCE, (b) PB-MWNTs-GCE, (c) DAR-CS/PB-MWNTs-GCE and (d) GOx/DAR-CS/PB-MWNTs-GCE in pH 6.5 PBS containing 10 mM  $K_3[Fe(CN)_6]/K_4[Fe(CN)_6]$ .

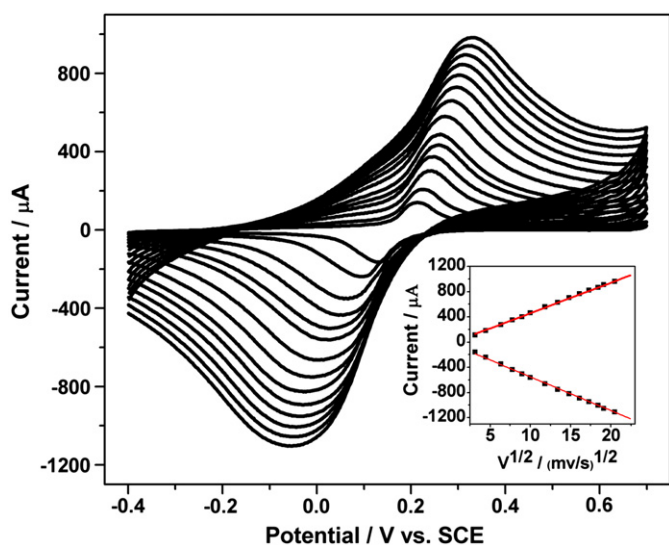


Fig. 4. Cyclic voltammograms of the GOx/DAR-CS/PB-MWNTs-GCE in pH 6.5 PBS at various scan rates. Inset: calibration plot of peak currents vs. scan rate.

illustrating that the intrinsic redox behavior of PB was well retained after the assembly of DAR-CS and GOx on the PB-MWNTs backbone.

The effect of pH value of PBS on electrochemical behavior of the GOx/DAR-CS/PB-MWNTs-GCE was studied as shown in Sfig. 1 in supporting information. With increasing the pH value of PBS in the range from 4.0 to 9.0, no apparent change was seen in the potential of the modified electrode. However, with the increase of pH value, both the  $I_{pc}$  and the  $I_{pa}$  decreased obviously. The result could be attributed to the well known fact that Prussian blue (PB) can be decomposed at alkaline conditions. Hence, in consideration of both the enzymatic activity and stability of PB, a weak acidic PBS with pH value of 6.5 was used in this work.

The analytical applications of most oxidase enzyme-based electrochemical biosensors were carried out by monitoring the enzymatically produced  $H_2O_2$  [21]. Fig. 5 shows the amperometric

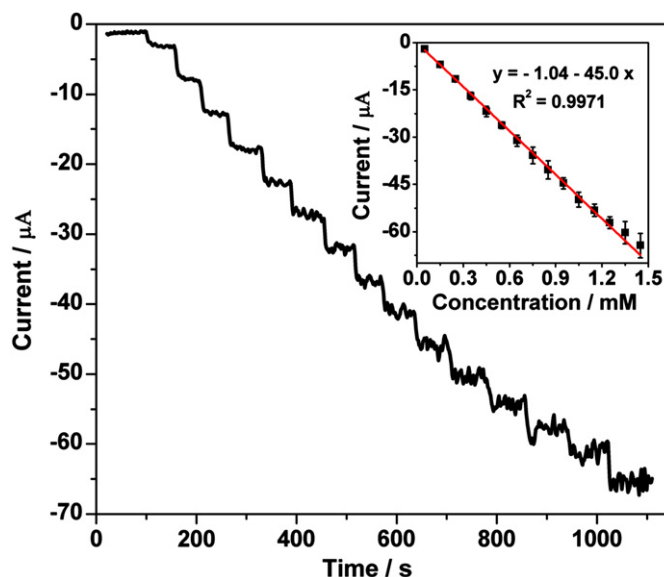
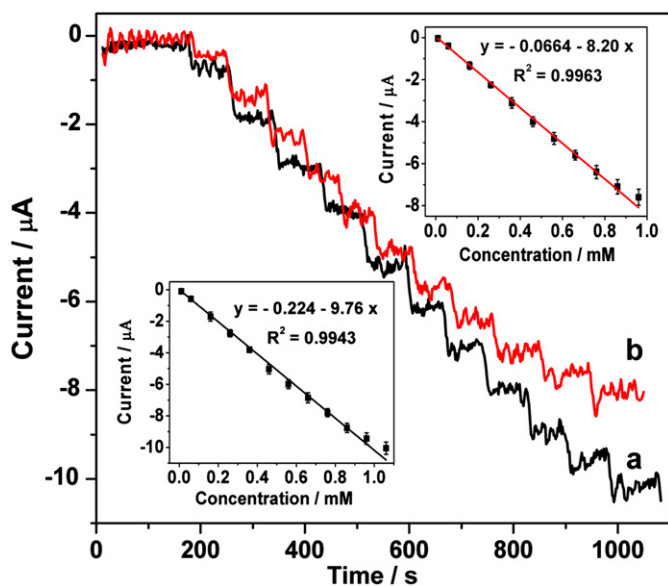


Fig. 5. Chronoamperometric response of the GOx/DAR-CS/PB-MWNTs-GCE in pH 6.5 PBS upon the successive addition of  $H_2O_2$  at  $-0.1$  V. Inset: calibration plot of response vs.  $H_2O_2$  concentration.

response of the GOx/DAR-CS/PB-MWNTs-GCE upon the successive addition of  $H_2O_2$  at  $-0.1$  V. The reduction current increased steeply and then reached 95% of the steady-state current within 10 s after the addition of  $H_2O_2$ . The linear response range to  $H_2O_2$  was from  $5.0 \times 10^{-5}$  to  $1.45 \times 10^{-3}$  M with a high sensitivity of  $358.4 \mu A mM^{-1} cm^{-2}$ . Because of its high selectivity and activity toward the reduction of  $H_2O_2$  in the presence of oxygen and other interferences, PB is usually considered as the “artificial enzyme peroxidase” [20,31]. The good amperometric response can be attributed to the synergistic effect of PB and MWNTs on the reduction of  $H_2O_2$ . The result indicated that the PB-MWNTs backbone can act as both the electron transfer facilitator and the low-potential electron transfer mediator for glucose biosensing based on the mediation toward the reduction of enzymatically produced  $H_2O_2$ . In addition, it had been reported that PB could mediate the oxidation of many other enzymatic products, such as thiocholine [32], indicating potential of the composite film in construction of a large number of other biosensors.

#### 3.4. Amperometric response of the biosensor to glucose

Fig. 6 shows the amperometric responses of the biosensors upon the successive addition of glucose at  $-0.1$  V. The GOx/DAR-CS/PB-MWNTs-GCE (a) showed a typical amperometric response to glucose. The time to reach 95% of the steady-state current was less than 10 s after the addition of glucose, indicating fast response of the biosensor. The linear response range to glucose was from  $1.0 \times 10^{-5}$  to  $1.1 \times 10^{-3}$  M with a correlation coefficient of 0.9943 and a sensitivity of  $77.9 \mu A mM^{-1} cm^{-2}$ . The detection limit was calculated to be  $3.1 \times 10^{-6}$  M defined from a signal/noise ratio of 3. More importantly, it was noteworthy that the sensitivity of the biosensor was higher comparing with that of other reported PB-MWNTs-based biosensors, such as the PB-MWNTs-CS-GOx-SiO<sub>2</sub>-GCE ( $15.2 \mu A mM^{-1} cm^{-2}$ ) [21] and the Nafion/GOx/PtCo nano-chains/PB-MWNTs-CS-GCE ( $21.0 \mu A mM^{-1} cm^{-2}$ ) [33]. The result can be attributed to the synergistic effect of efficient enzyme immobilization and good electrochemical properties of the GOx/DAR-CS/PB-MWNTs composite film. The uniform and highly porous feature of the PB-MWNTs forming membrane provided an opportunity for the deposition of large amounts of GOx on the PB-MWNTs backbone, and facilitated the diffusion of glucose into



**Fig. 6.** Chronoamperometric responses of (a) GOx/DAR-CS/PB-MWNTs-GCE and (b) GOx/DAR/PB-MWNTs-GCE in pH 6.5 PBS upon the successive addition of glucose at  $-0.1$  V. Inset: corresponding calibration plots of response vs. glucose concentration.

the composite film. PB-MWNTs as the assembly backbone offered the composite film both high electrical conductivity and efficient electron transfer mediation toward the reduction of enzymatically produced  $H_2O_2$ .

In addition, the GOx/DAR/PB-MWNTs-GCE fabricated without the use of CS in the composite film was also studied to evaluate the effect of CS on biosensing performance. The GOx/DAR/PB-MWNTs-GCE (b) showed a similar amperometric response to that of the GOx/DAR-CS/PB-MWNTs-GCE (a) except a much lower sensitivity of  $65.3 \mu A mM^{-1} cm^{-2}$ . The result implied that the involvement of CS to the composite film played an important role in the biosensing performance. As a well known biopolymer for enzyme immobilization due to its good biocompatibility, CS may provide a biocompatible microenvironment for immobilized GOx, which could greatly favor their enzymatic activity [34,35].

### 3.5. Stability of the biosensor

To evaluate the enzyme immobilization effectiveness of the composite film, the biosensing stability of the biosensor during the storage in vigorously stirred PBS at  $4^\circ C$  was studied. Fig. 7 shows variations of responses of the GOx/DAR-CS/PB-MWNTs-GCE without (a) and with (b) photo-cross-linking to  $0.1$  mM glucose with the storage time. As the storage time increased, the response of the biosensor without photo-cross-linking decreased drastically. The current response had decreased to about 50% of the initial response after the storage for 5 h, indicating poor biosensing stability of the biosensor. The poor biosensing stability illustrated poor structural stability of the non-photo-cross-linked GOx/DAR-CS/PB-MWNTs composite film. In the case of only the weak electrostatic interaction as the driving force for fabrication, the composite film was not stable during the storage [7], resulting in mass leakage of GOx from the PB-MWNTs backbone. Significantly, the biosensor with the photo-cross-linked GOx/DAR-CS/PB-MWNTs composite film showed much more stable response during the storage. More than 80% of the initial current retained after the storage for 5 h. The result demonstrated that the combination of the electrostatic self-assembly with the photo-cross-linking can dramatically improve the structural stability of the GOx/DAR-CS/PB-MWNTs composite

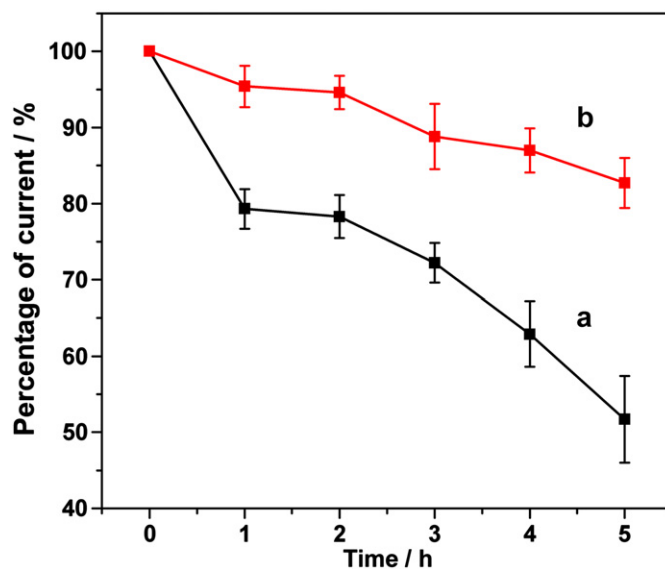


**Fig. 7.** Variations of chronoamperometric responses of the GOx/DAR-CS/PB-MWNTs-GCE fabricated (a) without and (b) with photo-cross-linking under UV irradiation for 3 min to  $0.1$  mM glucose with the storage time in vigorously stirred PBS at  $4^\circ C$ .

film. Due to the conversion of weak ionic bonds to strong covalent ones in the composite film, the leakage of enzyme can be effectively prevented, leading to greatly improved biosensing stability of the biosensor.

### 3.6. Reproducibility and anti-interference of the biosensor

The reproducibility of the biosensor was studied by successively detecting  $0.1$  mM glucose for 6 times, and the RSD of responses was 4.34%, demonstrating a good reproducibility. In addition, the RSD of responses to  $0.1$  mM glucose at five independently prepared biosensors was 5.71%, which proved good reproducibility of the biosensor preparation.

The addition of  $0.1$  mM uric acid and  $0.1$  mM ascorbic acid had no apparent influence on the response of the biosensor to  $0.1$  mM glucose, indicating high anti-interference ability of the biosensor. Because of its high selectivity and activity toward the reduction of the enzymatically produced  $H_2O_2$  in the presence of oxygen and other interferences [20], the PB-MWNTs backbone can act as a highly selective low-potential electron transfer mediator toward the reduction of enzymatically produced  $H_2O_2$ .

### 3.7. Glucose determination in real serum samples

To evaluate the ability of the biosensor in practical analytical applications, the biosensor was applied to determine the glucose concentration in fetal bovine serum samples. The glucose concentration in a fetal bovine serum sample was determined to be  $4.37 \pm 0.09$  mM by the biosensor, in good agreement with the value of  $4.56 \pm 0.05$  mM obtained using the traditional enzymatic method in a local hospital. In addition, the recovery test was carried out by adding  $0.1$  mM glucose to the serum samples, which produced a recovery of  $98.7 \pm 8.4\%$ , indicating good accuracy for the determination of glucose in real blood serum samples.

## 4. Conclusions

A novel glucose biosensor was fabricated based on electrostatic self-assembly in combination with in situ photo-cross-linking of

GOx as the model enzyme and DAR–CS on PB–MWNTs backbone. The PB–MWNTs backbone acted as both the electron transfer facilitator and the low-potential electron transfer mediator. The conversion of weak ionic bonds to strong covalent ones for enzyme immobilization by the combination of electrostatic self-assembly with photo-cross-linking resulted in highly stable immobilization of GOx. The biosensor showed excellent stability, high sensitivity, fast response time, good anti-interference ability, and acceptable ability in practical analytical applications due to synergistic effect of efficient enzyme immobilization and good electrochemical properties of the composite film fabricated by the proposed strategy. It should be noted that only negatively charged enzymes could be deposited onto the DAR–CS modified surface. Nevertheless, the strategy provided a promising platform for constructing a large number of other biosensors.

### Acknowledgments

This research was financially supported by National Natural Science Foundation of China (NSFC-20977021 and 30970829).

### Appendix A. Supplementary material

Supplementary data associated with this article can be found in the online version at <http://dx.doi.org/10.1016/j.talanta.2012.04.059>.

### References

- [1] N.J. Ronkainen, H.B. Halsall, W.R. Heineman, *Chem. Soc. Rev.* 39 (2010) 1747.
- [2] A.I. Gopalan, K.P. Lee, D. Ragupathy, S.H. Lee, J.W. Lee, *Biomaterials* 30 (2009) 5999.
- [3] Y. Zou, C. Xiang, L.X. Sun, F. Xu, *Biosens. Bioelectron.* 23 (2008) 1010.
- [4] M.L. Moraes, N.C. de Souza, C.O. Hayasaka, M. Ferreira, U.P. Rodrigues, A. Riul, V. Zucolotto, O.N. Oliveira, *Mater. Sci. Eng., C* 29 (2009) 442.
- [5] F. Lisdat, R. Dronov, H. Mohwald, F.W. Scheller, D.G. Kurth, *Chem. Commun.* 3 (2009) 274.
- [6] M. Liu, X.L. Yue, Z.F. Dai, L. Xing, F. Ma, N.Q. Ren, *Langmuir* 23 (2007) 9378.
- [7] Y.Y. Sun, F. Yan, W.S. Yang, C.Q. Sun, *Biomaterials* 27 (2006) 4042.
- [8] H. Zhu, M.J. McShane, *Langmuir* 21 (2005) 424.
- [9] B. Li, T.B. Cao, W.X. Cao, Z.J. Shi, Z.N. Gu, *Synth. Met.* 132 (2002) 5.
- [10] T.B. Cao, S.M. Yang, J. Cao, M.F. Zhang, C.H. Huang, W.X. Cao, *J. Phys. Chem. B* 105 (2001) 11941.
- [11] X. Shangguan, H.F. Zhang, J.B. Zheng, *Electrochem. Commun.* 10 (2008) 1140.
- [12] C.L. Fu, W.S. Yang, X. Chen, D.G. Evans, *Electrochem. Commun.* 11 (2009) 997.
- [13] F. Xi, L. Liu, Z. Chen, X. Lin, *Talanta* 78 (2009) 1077.
- [14] H. Zhong, R. Yuan, Y. Chai, W. Li, X. Zhong, Y. Zhang, *Talanta* 85 (2011) 104.
- [15] F. Li, J. Song, F. Li, X. Wang, Q. Zhang, D. Han, A. Ivaska, L. Niu, *Biosens. Bioelectron.* 25 (2009) 883.
- [16] Y. Liu, M. Wang, F. Zhao, Z. Xu, S. Dong, *Biosens. Bioelectron.* 21 (2005) 984.
- [17] M.P. O'Halloran, M. Pravda, G.G. Guilbault, *Talanta* 55 (2001) 605.
- [18] W. Li, R. Yuan, Y. Chai, *Talanta* 82 (2010) 367.
- [19] A. Ahmadalinezhad, A.K.M. Kafi, A.C. Chen, *Electrochem. Commun.* 11 (2009) 2048.
- [20] J. Li, J.D. Qiu, J.J. Xu, H.Y. Chen, X.H. Xia, *Adv. Funct. Mater.* 17 (2007) 1574.
- [21] G.L. Fu, X.L. Yue, Z.F. Dai, *Biosens. Bioelectron.* 26 (2011) 3973.
- [22] J.F. Zhai, Y.M. Zhai, D. Wen, S.J. Dong, *Electroanalysis* 21 (2009) 2207.
- [23] Z.H. Yang, J.Y. Chen, W.X. Cao, *Polym. Int.* 53 (2004) 815.
- [24] J.H. Shi, Y.J. Qin, H.X. Luo, Z.X. Guo, H.S. Woo, D.K. Park, *Nanotechnology* 18 (2007) 365704.
- [25] H. Zhong, J.F. Wang, X.F.R. Jia, Y. Li, Y. Qin, J.Y. Chen, X.S. Zhao, W.X. Cao, M.Q. Li, Y. Wei, *Macromol. Rapid Commun.* 22 (2001) 583.
- [26] Z.H. Yang, T.B. Cao, J.Y. Chen, W.X. Cao, *J. Chem., Chinese Univ.* 23 (2002) 342.
- [27] D. Xu, C.J. Tsai, R. Nussinov, *Protein Eng.* 10 (1997) 999.
- [28] S. Yoshioki, *J. Comput. Chem.* 23 (2002) 402.
- [29] R.L. Jernigan, I. Bahar, *Curr. Opin. Struct. Biol.* 6 (1996) 195.
- [30] M. Tarek, D.J. Tobias, *Phys. Rev. Lett.* 88 (2002) 138101.
- [31] E. Nossol, A.J.G. Zarbin, *Adv. Funct. Mater.* 19 (2009) 3980.
- [32] F. Ricci, F. Arduini, A. Amine, D. Moscone, G. Palleschi, *J. Electroanal. Chem.* 563 (2004) 229.
- [33] X. Che, R. Yuan, Y.Q. Chai, J.J. Li, Z.J. Song, W.J. Li, *Electrochim. Acta* 55 (2010) 5420.
- [34] X. Kang, J. Wang, H. Wu, I.A. Aksay, J. Liu, Y. Lin, *Biosens. Bioelectron.* 25 (2009) 901.
- [35] G. Wang, J.J. Xu, H.Y. Chen, Z.H. Lu, *Biosens. Bioelectron.* 18 (2003) 335.